Polymer 51 (2010) 3503–3511

Contents lists available at ScienceDirect

Polymer

journal homepage: www.elsevier.com/locate/polymer

Thermotropic LCP/CNF nanocomposites prepared with aid of ultrasonic waves

Rishi Kumar, Avraam I. Isayev*

Institute of Polymer Engineering, The University of Akron, Akron, OH 44325-0301, USA

ARTICLE INFO

Article history:
Received 23 February 2010
Received in revised form
15 May 2010
Accepted 21 May 2010
Available online 1 June 2010

Keywords:
Ultrasound
Nanocomposites
Melt processing

ABSTRACT

Ultrasound assisted twin screw extrusion process was developed to disperse carbon nanofibers (CNFs) in a polymer matrix. CNFs were separately added into the melt stage to reduce the breakage of CNFs and to avoid intense stresses in the feed zone. The effect of ultrasound and CNFs loading on die pressure, rheological, mechanical, electrical and morphological properties of liquid crystalline polymer (LCP) filled with 0–20 wt% CNFs was studied. Ultrasonic treatment caused a reduction in die pressure and a decrease in electrical percolation threshold value of treated samples. It was also found that mechanical properties of ultrasonically treated LCP/CNF nanocomposite moldings were preserved, improved or slightly decreased in comparison with those of LCP. This is in contrast to available literature typically showing a deterioration of mechanical properties with addition of CNFs. SEM studies have indicated an improved dispersion of CNFs and a reduction of LCP rich area in nanocomposites upon ultrasonic treatment.

1. Introduction

High performance fiber-reinforced composites have been widely used in various engineering applications due to their light weight and high mechanical properties. Till date, carbon-fiber and glass-fiber composites dominate the industry. There are some limitations associated with the glass-fiber-reinforced composites such as the accumulation of electrostatic charge on their surface which can cause local heating resulting in the catastrophic failure of the surrounding materials. In recent years [1], polymer/CNF composites have gained a considerable attention both in academia and industry due to their exceptional electrical, thermal and mechanical properties along with their light weight. When these nanofibers are used as reinforcing materials in a polymer matrix, they provide superior electrical conductive properties as compared to the conventional fiber-reinforced composites [2]. Due to their high aspect ratio, it is possible to achieve percolation threshold at very low loading. A wide range of potential applications of these nanocomposites have been studied [3]. CNFs are produced by vapor grown carbon method, based on catalytic decomposition of hydrocarbons in the vapor phase at 500–1500 °C. However, during the synthesis, CNFs easily aggregate or form bundles due to strong interfiber attraction which hinders its homogeneous dispersion at the nanoscale level in the polymer matrix and hence limits their effective use. The dispersion of CNFs is a biggest challenge. A number of studies [4,5] have been done to disperse the CNFs, however, a homogeneous dispersion still remains a big challenge, as can be seen from review papers [1,6] on dispersion of CNFs in a polymer matrix. The commonly used methods to disperse CNFs in a polymer matrix are: in-situ polymerization, mechanical, chemical and plasma treatment [1,7]. Among these methods in-situ polymerization and chemical modification may not be commercially viable due to their limitation in scale up and their negative environmental impact. Prolonged sonication of the CNFs in ultrasonic bath using solvent is one of the most commonly used methods to disperse nanofibers. However, it introduces defects in CNFs and results in reduced aspect ratio which is basis for many of its attractive properties [8].

LCPs attracted a lot of attention due to their excellent mechanical and thermal properties with low oxygen/water permeability and making them promising material for high performance molding, optoelectronics and photonic devices [9,10]. LCP materials are characterized by long, rigid, rod-like molecules that get aligned in the elongational flow resulting in superior mechanical properties. LCP has very low conductivity, preventing their use in high performance applications where EMI shielding is desired. CNFs have been incorporated in many thermoplastics [11,12] to improve their electrical conductivity. However, limited studies have been done on LCP/CNF [13,14] and LCP/multiwalled carbon nanotube (MWCNT) [15] nanocomposites.

In study [13], LCP Vectra 400P and CNFs were subjected to intense mixing in Rheomixer for 20 min. An electrical percolation threshold was observed near the 5 wt% loading of CNF, however, the mechanical properties decreased significantly. In another study

* Corresponding author. Tel.: +1 330 972 6673.
E-mail address: aisayev@uakron.edu (A.I. Isayev).

0032-3861/$ – see front matter © 2010 Elsevier Ltd. All rights reserved.
doi:10.1016/j.polymer.2010.05.042

[14], LCP Vectra A 950 was compounded with CNFs in a twin screw extruder and extrudate monofilaments were collected. A little increase in mechanical properties was observed at 1 wt% loading. However, mechanical properties decreased significantly at higher loading of CNFs. In another study [15], carboxylated MWCNTs and LCP Zenite 6000 were processed in Haake rheometer. It was observed that mechanical properties slightly increased at 0.1 wt% loading and start decreasing at higher nanotubes loading. From the above discussion, it has been observed that to achieve the homogenous dispersion of CNFs in high performance and viscous materials is a challenging task. So there is a clear need to develop a new clean, rapid and environment friendly method which can process highly viscous materials.

Over the past decade extensive work has been done to develop a novel extrusion process with the aid of high power ultrasound [16–20]. A number of studies on the effect of ultrasound on polymers have been published and reported in various review articles and books. It was shown that ultrasonic oscillations can breakdown the 3-D network in vulcanized rubber within seconds. Ultrasound was found to improve the compatibilization of immiscible plastic blends, plastics/rubber and rubber/rubber blends during extrusion process [21]. In recent years, use of ultrasound to disperse nanofiller in a polymer matrix is gaining attention. Ultrasound helps in continuous dispersion of CNFs and carbon nanotubes in high performance polymer matrix [22,23].

To our knowledge, there has been no work done to improve the dispersion of CNFs in LCP matrix with the help of ultrasound assisted extrusion process. Therefore, this work presents a novel method for the continuous dispersion of CNFs in a polymer matrix. Ultrasound assisted twin screw extrusion of LCP/CNF has been carried out by feeding CNF into molten LCP stream. This is in contrast to earlier studies where polymers physically premixed with CNF were fed to the extruder [22,23]. LCP was chosen because of its excellent chemical resistance, mechanical and thermal properties. They have outstanding dimensional and thermo-oxidative stability with desired processability required for space applications. The effects of ultrasound on die pressure, electrical conductivity, rheological, morphological and mechanical properties were studied.

2. Experimental

2.1. Materials

LCP used was wholly aromatic copolyester containing 73% HBA (1,4-dihydroxybenzoic acid) and 27% HNA (2,6-dihydroxynaphthoic acid). It was in pellet form, made by Celanese and marketed by Ticona under trade name Vectra A 950. It has the melting temperature of 275 °C. The CNFs, Pyrograf-III, were provided by Applied Sciences, Inc., Cedarville, OH. They were used as received. These nanofibers were vapor grown and heat treated upto 3000 °C to increase their electrical conductivity. The CNFs had a diameter of 70–200 nm and length varied from 50 to 100 μm.

2.2. Preparation and characterization of LCP/CNF nanocomposite

The LCP pellets and CNFs were dried separately in a vacuum oven at 110 °C for at least 24 h prior to processing. For melt processing, a continuous co-rotating twin screw extruder equipped with high power ultrasonic die attachment was used as shown in Fig. 1. The details about the design of ultrasonic slit die and ultrasonic attachment can be found in previous study [23]. In contrast to the earlier study where a physical mixture of the polymer and nanofillers were fed into feed section of the extruder, whereas in the present study LCP was fed into feed section while CNFs were fed into LCP stream after melting. The microextruder (PRISM USA LAB 16, Thermo Electron Corp., UK) has diameter of 16 mm with $L/D = 25$. Two pressure transducers (TPT 412-5M-6/18, Dynisco Instruments, Franklin, MA) of maximum pressure of 5000 psi, were placed in the die zone immediately before and after the ultrasonic treatment zone. The die pressure and temperature were recorded by data acquisition system (Dataq Instruments, DI-715-U, Akron, OH). Two horns oscillating at a frequency of 40 kHz were attached to the die zone having a 4 mm gap size for flow of polymer melt. The molten compound was continuously subjected to amplitudes ranging from 0 to 3.2 μm. Dried LCP pellets were fed to the extruder using a twin screw feeder (K-Tron Soder, Model K2V-T20, Pitman, NJ, USA). A separate high precision feeder (Brabender Technology MT-2, Germany) was used to add the CNFs in the melt to reduce the breakage of nanofibers due to high stresses in the feed zone. The temperature in the barrel section was set from feed zone to die zone as 300 °C. The screw speed was set at 150 rpm. The feed rate of LCP pellets and CNFs were adjusted to give output of 1 lb/h of nanocomposites. Extruded nanocomposites were dried and pelletized in a grinder (Weima America Inc., Fort Mill, SC).

Prepared nanocomposites were compression molded into discs of 25 mm diameter and 2.2 mm thickness at 300 °C using the compression molding press (CARVER 4122, Wabsah, IN) for the rheological measurements. Advanced Rheometric Expansion System (Model ARES LS, TA instruments) was used to study the rheological properties of the nanocomposites. A 25 mm parallel plate geometry in oscillatory shear mode with dynamic frequency sweep test was used at 300 °C and a fixed strain amplitude of 2%. The studied frequency range was 0.03 rad/s to 100 rad/s. The complex viscosity, storage modulus, loss modulus and loss tangent were obtained as a function of the angular frequency. The disc shaped sample was placed between the heated parallel plates and squeezed and then excess material was removed from the sides to remove any boundary effects. Data acquisition was carried out with the aid of a microcomputer interfaced with the rheometer.

The samples for electrical conductivity measurements were also compression molded at 300 °C into discs of 90 mm diameter and 1 mm thickness. An electrometer, Keithley Instrument (Model 6517 A, Keithley Instruments, Cleveland, OH) attached to an 8009 test fixture was used to measure the volume resistivity of the prepared samples in accordance with ASTM D257 method. The measurements were done at a constant voltage of 1.0 and 0.1 V. The readings were taken 60 s after the applied voltage to get the stabilized values. At high applied voltage, materials having high CNFs loadings become very conductive and cause the short circuiting of the electrometer. Hence, it was difficult to measure the volume resistivity for all samples at same high voltage. The low voltage of 1.0 and 0.1 V was chosen for the comparison purpose and to show the effect of voltage on percolation threshold value as different voltages can lead to different percolation threshold values.

Specimens for tensile test were prepared according to ASTM D-638 using the HAAKE mini-jet piston injection molder (HAAKE, Thermo Electron Corp., Germany) at a melt temperature of 290 °C and mold temperature of 80 °C. The injection pressure was 420 bars in each case. High temperature mold release agent (Frekote HMT2) was sprayed before injecting the material.

The oriented fibers of LCP/CNF nanocomposites were prepared using capillary rheometer (Rosand 2000). The barrel temperature of 300 °C was used to produce the fibers. As the rod-like strand comes out of the capillary die of a diameter of 2 mm and $L/D = 32$, it was stretched and collected at ambient air cooling using a cylindrical take up device. Three different draw down ratios (DDR) were used to produce the fibers of different diameters at a flow rate of 15 g/min. The three DDR used were 30, 51 and 75. The fibers of LCP/CNF nanocomposites upto 5 wt% CNFs loadings were melt spun;

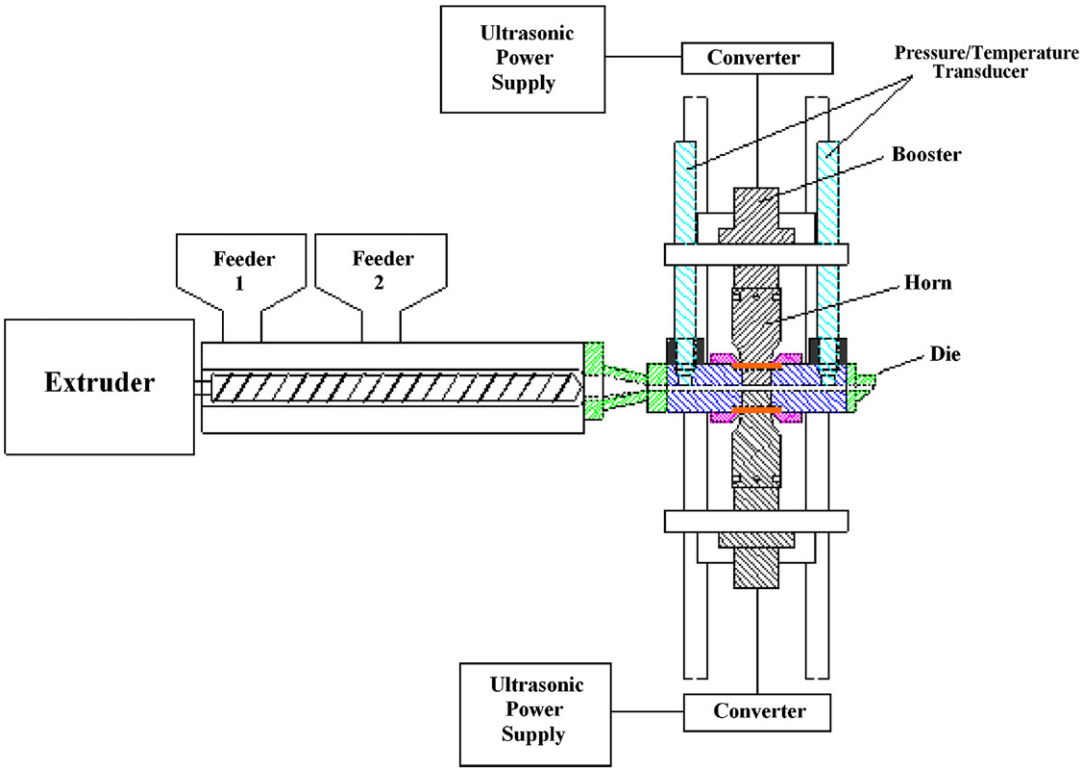

Fig. 1. The ultrasonic twin screw microextruder.

however the higher CNFs loadings fibers were difficult to prepare due to melt fracture and high viscosity of the polymer melt.

Instron tensile testing machine (Model 5567, Instron Corp., Canton, MA) was used to carry out the tensile tests on injection molded tensile bars and melt spun fibers at room temperature. The injection molded samples were clamped in the jaws of the testing machine and put under tension using a 10 kN load cell. In case of tensile testing of fibers, a single fiber was tested for every condition using a 100 N load cell. Tests were carried out according to ASTM D-638 test method using an extensometer at a cross-head speed of 5 mm/min. A minimum of five samples were tested for both injection molded bars and melt spun fibers for each condition. The Young's modulus, tensile strength and yield strain were measured. The average and standard deviation of obtained values were calculated.

The effect of ultrasonic wave on the state of dispersion of carbon nanofibers in an LCP matrix can be best visualized using microscopic studies. Scanning electron microscope (Hitachi S-2150 SEM at 20 kV) was used to study the surface morphology and state of dispersion of CNFs. For microscopic studies, cryofractured compression molded disc shape samples without any silver sputter coating were used.

3. Results and discussion

3.1. Process characteristic

The die pressure before the ultrasonic attachment zone of LCP/CNF nanocomposites at various loadings of CNFs as a function of ultrasonic amplitude during the extrusion of LCP/CNF nanocomposites is presented in Fig. 2. The die pressure increases with increasing CNFs content, as expected, due to increase in viscosity caused by increase in CNFs content. A continuous decrease in die pressure with ultrasonic amplitude was observed. This decrease in die pressure becomes more efficient with an increase of concentration of CNF. This could be due to occurrence of acoustic cavitation phenomenon in the melt leading to the both permanent and thixotropic changes in the melt [16]. These effects of ultrasonic cavitation on the chain scission of the polymer matrix were not observed, as will be seen from the Fig. 3 below, where no significant decrease in complex viscosity occurs upon application of ultrasound. However, degradation of matrix in the presence of CNFs cannot be ruled out, as the possibility of a local energy density at the interfaces between polymer and CNFs may exist. The possible shear thinning behavior of the melt may get enhanced on application of ultrasonic

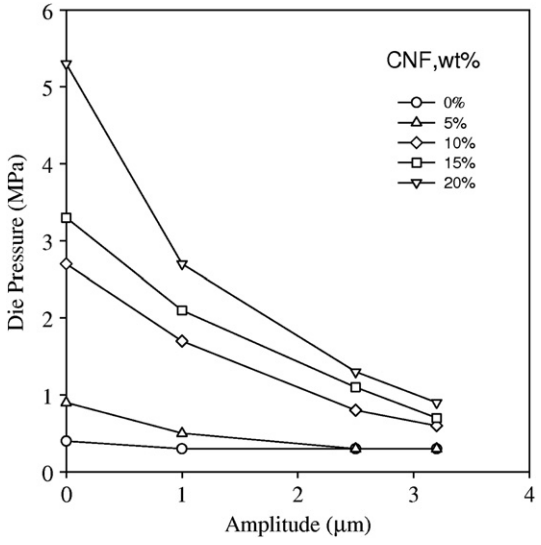

Fig. 2. Die pressure versus amplitude at different CNF loadings.

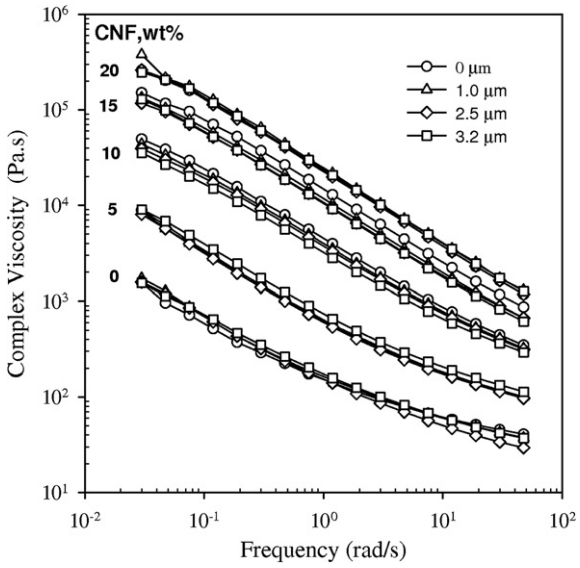

Fig. 3. Complex viscosity as a function of frequency at different ultrasonic amplitudes and CNF loadings.

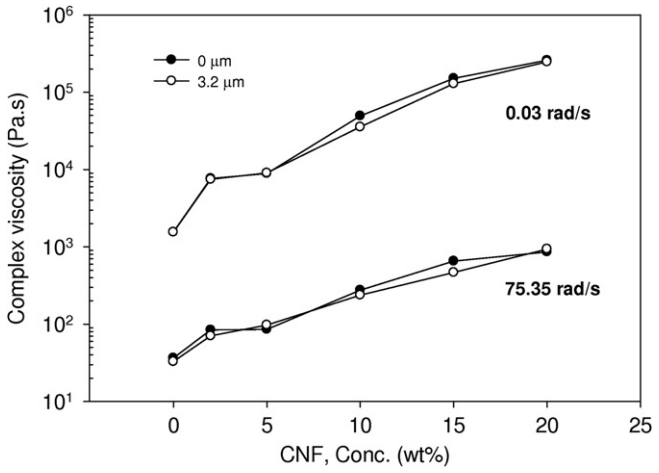

Fig. 4. Complex viscosity versus CNF concentration at frequencies of 0.03 rad/s and 75.35 rad/s for untreated and ultrasonically treated nanocomposites at an amplitude of 3.2 μm.

waves leading to temporary decrease in melt viscosity that recovers after treatment. In addition to shear thinning and thixotropic changes, the reduction in die pressure is due to combination of heating from dissipated energy from ultrasound and reduction in friction at horn surfaces due to ultrasonic vibrations [16].

3.2. Rheology

Fig. 3 shows the complex viscosity of nanocomposites as a function of frequency at different CNF loadings for untreated and ultrasonically treated samples. It can be seen that there is continuous increase in the complex viscosity with the increase of CNFs loadings. The complex viscosity was increased by more than 2 orders of magnitude on an addition of 20 wt% of CNFs. Such a large increase in viscosity with CNF concentration does not conform with corresponding smaller increase of die pressure. This inconsistency on behavior of die pressure is apparently due to the presence of slip effects during flow throughout the die even in the absence of ultrasonic treatment. The decrease in viscosity with the increase of frequency indicates the non-Newtonian behavior of nanocomposites. A stronger shear thinning behavior was observed at higher CNFs loadings as compared to at low CNFs loadings. The orientation of the domains and rigid molecular chains in LCP on application of shear force results in increase of shear thinning behavior of nanocomposites. The behavior is in accordance with the earlier studies on PEI/CNF and PEI/CNT nanocomposites [22,23]. This increase in viscosity does not affect the processability of the melt as ultrasonic treatment helps in processability with decrease in die pressure as explained previously in process characteristic. By comparing die pressure and complex viscosity variations with amplitude one can see that the viscosity changes less with amplitude than the die pressure. This observation led us to believe that significant reduction of die pressure with ultrasonic amplitude in these LCP/CNF nanocomposites is due to thixotropic effects and a possible slippage on the horn surface.

The existence of rheological percolation threshold can be understood by plotting complex viscosity versus CNF concentration at low (0.03 rad/s) and high (75.35 rad/s) frequencies for untreated and ultrasonically treated samples at an amplitude of 3.2 μm, as shown in Fig. 4. A sudden increase in the complex viscosity is observed on an addition of 2 wt% of CNF indicating the possibility of occurrence of rheological percolation threshold at low concentration in comparison with the electrical percolation discussed later.

Both the storage (G') and loss (G'') moduli of LCP and their nanocomposites increased with the increase of frequency (ω) (Fig. 5). There was tremendous increase in the storage and loss modulus of nanocomposites with the increase of the CNF loadings. It was observed that as the CNF loadings increased the slope of the G' and G'' vs. ω curves keep changing and getting less steeper (approaching a plateau) at intermediate frequencies indicating the existence of interconnected structure of CNFs which are an anisotropic filler [24]. At low frequencies, similar to earlier observations on PEI/MWNT nanocomposites [23], some drop in G' values was observed with frequency. The effect of ultrasound and CNFs loadings on the structural differences between the polymer and the nanocomposites can be seen from the logarithmic plot of G' vs. G'' (Fig. 6), which is similar to Cole–Cole plot. Curves without and with ultrasonic treatment at each concentration of CNF practically coincide indicating no significant changes in the molecular structure of LCP and nanocomposites due to ultrasonic treatment. It can also be seen that at a given G'' value, there is a significant increase in G' value with the increase of CNFs loadings. This behavior is in accordance with earlier studies reported on PEI/CNF [22], PEI/MWNT [23], PC/MWNT [24] and HDPE/MWNT [25] nanocomposites where similar behavior was observed on addition of CNT and CNF to the polymer matrices.

The effect of ultrasound and CNF loading on the tan δ can be seen by plotting tan δ versus frequency at different CNF loadings for untreated and ultrasonically treated samples at 3.2 μm (Fig. 7). It is observed that tan δ decreased with addition of CNF and the effect is more pronounced at higher frequency as compared to lower frequency, indicating that the relaxation behavior of polymer chains strongly get affected with CNF content. At low level of CNF loadings and high frequency the value of tan δ seems to be higher than that at the lower frequency. This is opposite to the behavior at high loading and at low frequency where tan δ value is higher. The ultrasonically treated samples do not show significant differences in value of tan δ as compared to the untreated samples at all CNF concentrations.

Ultrasound does help in the dispersion of the CNFs as seen from the morphological studies discussed in later part of this study. The increase in ultrasonic amplitude does not significantly affect the complex viscosity of the LCP/CNF nanocomposites, as seen from

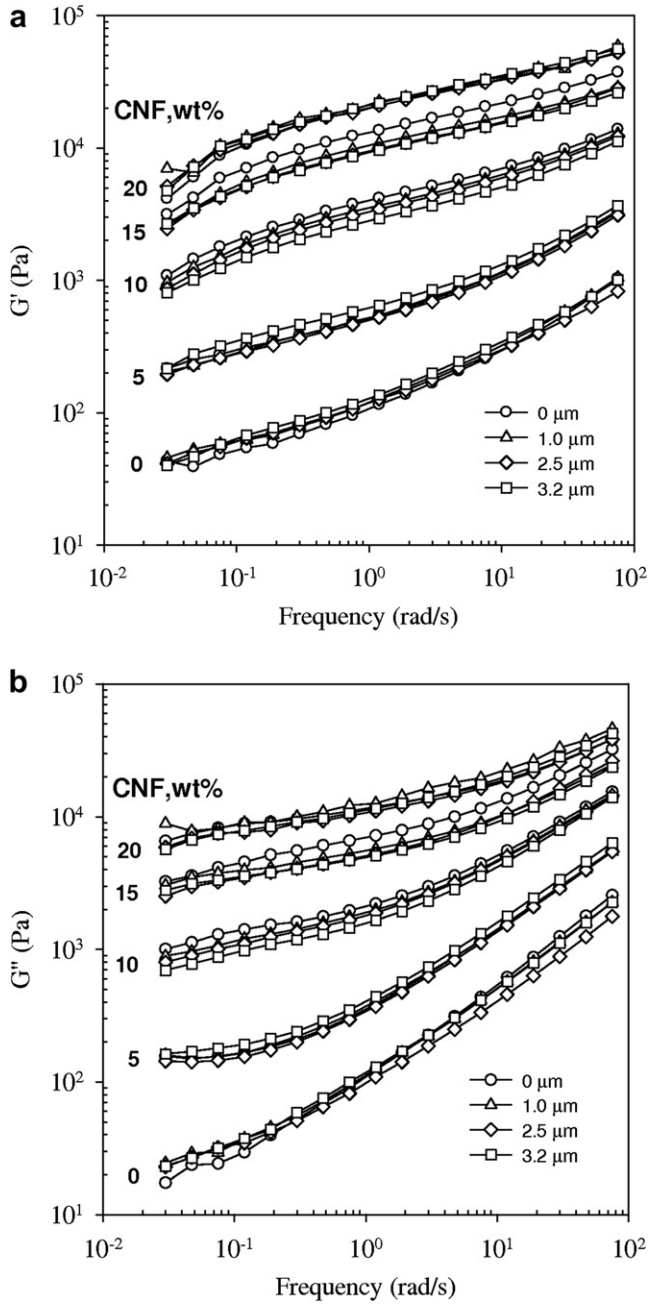

Fig. 5. Storage (a) and loss (b) moduli as a function of frequency at different ultrasonic amplitudes and CNF loadings.

Figs. 3 and 4. However, the fibrillation structure of LCP apparently gets affected with increased dispersion. Therefore, this increased dispersion practically does not affect the rheological behavior of LCP/CNF nanocomposites, possibly, due to a reduction in fibrillation of LCP matrix in the presence of CNFs. In fact, in PEI/CNF [23] and PEI/MWNT [24] nanocomposites, where matrix does not fibrillate and dispersion of nanofillers was improved due to ultrasonic treatment, a significant increase of viscosity was observed resulting in permanent changes in rheological behavior.

3.3. Electrical resistivity

CNFs being highly electrically conductive fillers were added to the insulating LCP matrix to improve its electrical conductivity. A

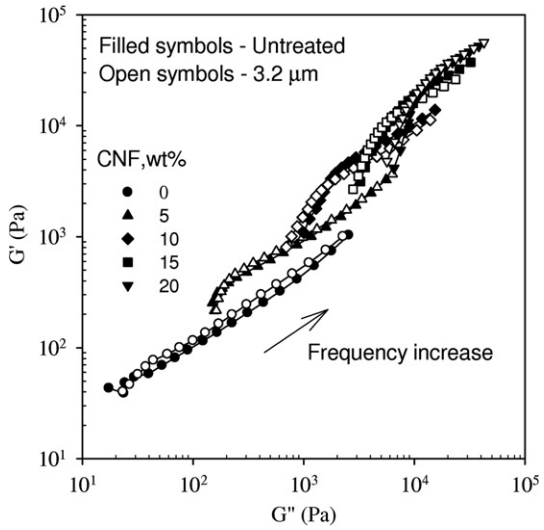

Fig. 6. G' versus G'' for untreated and ultrasonically treated nanocomposites at an amplitude of 3.2 μm and at various CNF loadings.

critical loading of CNFs is required where the interconnected network of CNFs formed resulting in creation of conductive path causing the material to behave like a conductor. This critical loading is termed as the percolation threshold, below which the conductivity of the nanocomposite is close to the conductivity of unfilled material. Above the percolation threshold a sharp reduction in resistivity occurred making it conductive and suitable for certain applications where electrical conductivity is required. Once the percolation threshold reached, there is not much decrease in the resistivity on a further addition of nanofibers and conductivity levels off and attains the value of conductive particles.

Fig. 8 shows the volume resistivity of the nanocomposites as a function of CNFs loading at different ultrasonic amplitudes and at 1.0 V (a) and 0.1 V (b). The volume resistivity decreased by over 3 and 4 orders of magnitude with 10 wt% CNFs loading without and with ultrasonic treatment at an amplitude of 3.2 μm (Fig. 8a). A sharp reduction in resistivity is observed between 5 and 10 wt% CNFs loading indicating the percolation threshold lies between 5 and 10 wt % loading. The resistivity further decreased by an order of magnitude

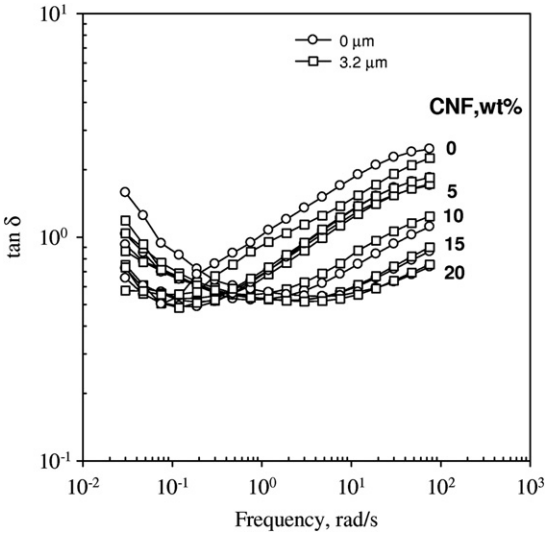

Fig. 7. tan δ as a function of frequency for untreated and ultrasonically treated nanocomposites at an amplitude of 3.2 μm and at various CNF loadings.

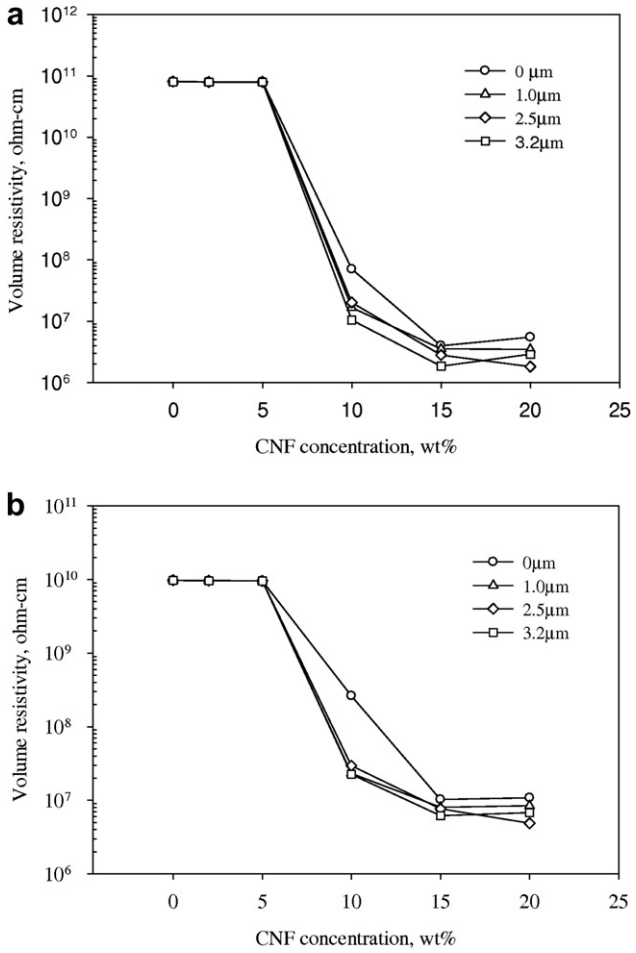

Fig. 8. Volume resistivity at 1.0 V (a) and 0.1 V (b) as a function of CNF concentration at various ultrasonic amplitudes.

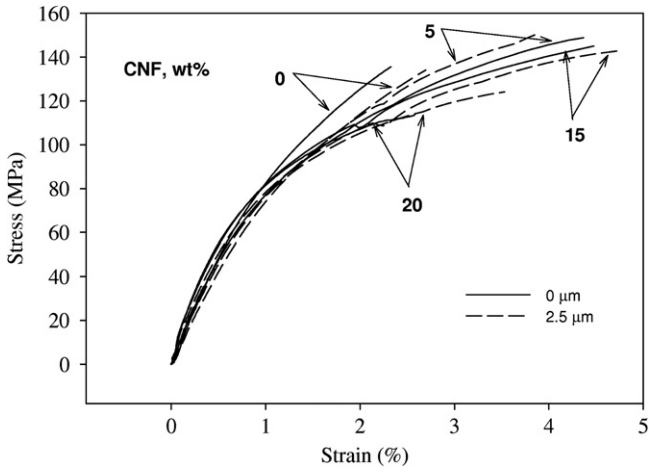

Fig. 9. Stress–strain curves for LCP and LCP/CNF nanocomposite moldings untreated and ultrasonically treated at an amplitude of 2.5 μm and at various CNF loadings.

on addition of 15 wt% of CNFs. Once the percolation threshold was achieved, a little drop in resistivity was observed on further increasing the CNFs content upto 20 wt%. For untreated nanocomposites at 0.1 V, the volume resistivity dropped by about 2 orders of magnitude at 10 wt% CNFs loading, whereas, for the ultrasonically treated samples, this drop in volume resistivity was about 3 orders of magnitude at same CNFs loading, as can be seen from Fig. 8b. Therefore, an order of magnitude drop in volume resistivity of nanocomposites was observed due to ultrasonic treatment alone at same CNF loading and different voltages. Also, it should be noted that different voltages provide different conductivity values. Therefore, for comparison purpose measurements were done at low voltages, as it was difficult to take measurements at high voltages for the samples of high CNF loadings since the electrometer gets tripped off. Fig. 8 indirectly indicates that high power ultrasonic treatment helps in improving the dispersion of CNFs in a polymer matrix and at the same time leading to the formation of better interconnected network of CNFs and, hence, resulting in improved electrical conductivity. The results are in accordance with the earlier study carried on PEI/CNFs nanocomposites [22], where the percolation threshold falls to 15 wt% of CNFs loadings for ultrasonically treated nanocomposites as compared to the 18 wt% of CNFs loadings for untreated nanocomposites. LCP nanocomposites reached percolation threshold at lower CNFs loadings as compared to other thermoplastics. Lozano et al. [11] found the electrical percolation to be at 20 wt% of CNFs loading for PP/CNFs nanocomposites. A possible reason for lower values of percolation in LCP is the self-aligning nature of their domains which get oriented under shear flow and tend to align nanofibers bringing them close to each other resulting in conductive material at much lower loading [10]. It was observed that both rheological and electrical percolation threshold values differ from each other as can be seen from Figs. 4 and 8, with rheological threshold values being lower than the electrical ones. This is in contrary to earlier study done on PEI/MWNT nanocomposite prepared by similar processing method where both rheological and electrical percolation threshold values lie in the same range. However, a number of other studies [26–28] also suggested the difference in value of rheological and electrical percolation threshold values.

From the available literature, it seems that the electrical percolation threshold is highly dependent on the nature of polymer or the

Table 1
Mechanical properties of LCP and LCP/CNF nanocomposite moldings at different CNFs loadings and ultrasonic amplitudes.

CNF (wt%)	Ultrasonic amplitude (μm)	Young's modulus (GPa)	Tensile strength (MPa)	Elongation at break (%)
0%	0	9.97 ± 0.41	135.7 ± 9.96	2.34 ± 0.42
	1	9.94 ± 0.09	142.0 ± 2.31	2.12 ± 0.55
	2.5	9.54 ± 1.03	136.0 ± 13.8	2.65 ± 0.82
	3.2	10.06 ± 0.68	139.0 ± 9.09	2.51 ± 0.82
2%	0	9.66 ± 0.33	144.0 ± 14.0	3.12 ± 0.76
	1	9.62 ± 0.6	143.7 ± 3.3	3.16 ± 0.74
	2.5	9.29 ± 0.38	140.2 ± 6.3	2.99 ± 0.46
	3.2	9.98 ± 0.81	120.2 ± 15.8	2.48 ± 1.16
5%	0	9.83 ± 1.3	141.38 ± 18.5	4.37 ± 0.62
	1	8.55 ± 0.64	151.7 ± 5.92	4.59 ± 0.77
	2.5	9.29 ± 0.94	152.8 ± 9.3	3.77 ± 0.72
	3.2	9.54 ± 0.86	130.4 ± 9.75	2.52 ± 0.35
10%	0	9.49 ± 0.4	150.4 ± 8.39	4.61 ± 0.84
	1	9.25 ± 0.42	146.8 ± 4.7	4.54 ± 0.97
	2.5	8.96 ± 0.51	139.6 ± 12.5	4.22 ± 1.03
	3.2	8.92 ± 0.5	139.0 ± 13.3	4.22 ± 1.1
15%	0	9.85 ± 0.66	144.1 ± 3.45	4.47 ± 0.6
	1	9.67 ± 0.47	146.1 ± 2.8	5.16 ± 0.42
	2.5	9.31 ± 0.19	139.0 ± 9.72	4.81 ± 1.01
	3.2	9.89 ± 0.31	137.8 ± 6.6	4.05 ± 0.87
20%	0	10.09 ± 0.45	111.3 ± 14.0	2.59 ± 1.02
	1	10.05 ± 0.53	125.9 ± 12.7	3.6 ± 1.13
	2.5	9.5 ± 0.75	122.2 ± 6.6	3.6 ± 1.23
	3.2	9.9 ± 0.26	118.1 ± 11.3	2.75 ± 0.77

process used. For a material to be electrically conductive, CNFs are not required to touch each other in order to make the network providing the percolation threshold. However, it is sufficient for CNFs to be close to each other such that electron hopping between CNFs could take place. For the occurrence of hopping process the distance between CNFs should be less than 5 nm to make electrically conductive network. On the other hand, in the case of the rheological percolation threshold, as long as the distance between CNFs is comparable with the radius gyration of polymer molecules (which is about tens of nanometers), it can restrict the mobility of polymer chains at the local level [26,27]. Hence, the distance between CNFs to achieve rheological percolation is less than that required for electrical percolation threshold. Therefore, a fewer CNFs are required to achieve rheological percolation threshold.

3.4. Mechanical properties

Fig. 9 shows the typical stress–strain curves for the LCP/CNF nanocomposites at different CNFs loadings and at constant ultrasonic amplitude of 2.5 μm. In general, the composites are known to become brittle on an addition of fibers. However, in the present study it was observed that shape of the stress–strain curve did not change even on an addition of 20 wt% CNFs, as can be seen from Fig. 9. On contrary the elongation at break increases in the presence of high amount of CNFs.

The effect of ultrasonic treatment and CNFs loadings on the Young's modulus, tensile strength and elongation at break of LCP/CNF nanocomposites is shown in Table 1. In general, no significant change in the Young's modulus and tensile strength of the LCP/CNF nanocomposites were observed on an addition of CNFs and on application of ultrasound. However, a reduction in the tensile strength of the LCP/CNF nanocomposite was observed at 20 wt% of CNF loading. Surprisingly, the elongation at break of the nanocomposites increased with the CNF loading in comparison with pure LCP. Some reduction in the elongation at break was observed at 20 wt% of CNFs loading but its value is still higher than that of pure LCP. LCPs are unique in their flow behavior, as compared to conventional thermoplastics. LCPs form domains in the melt state which get oriented and fibrillated in the elongational flow such as occurs in fiber spinning or extrusion process. The latter leads to

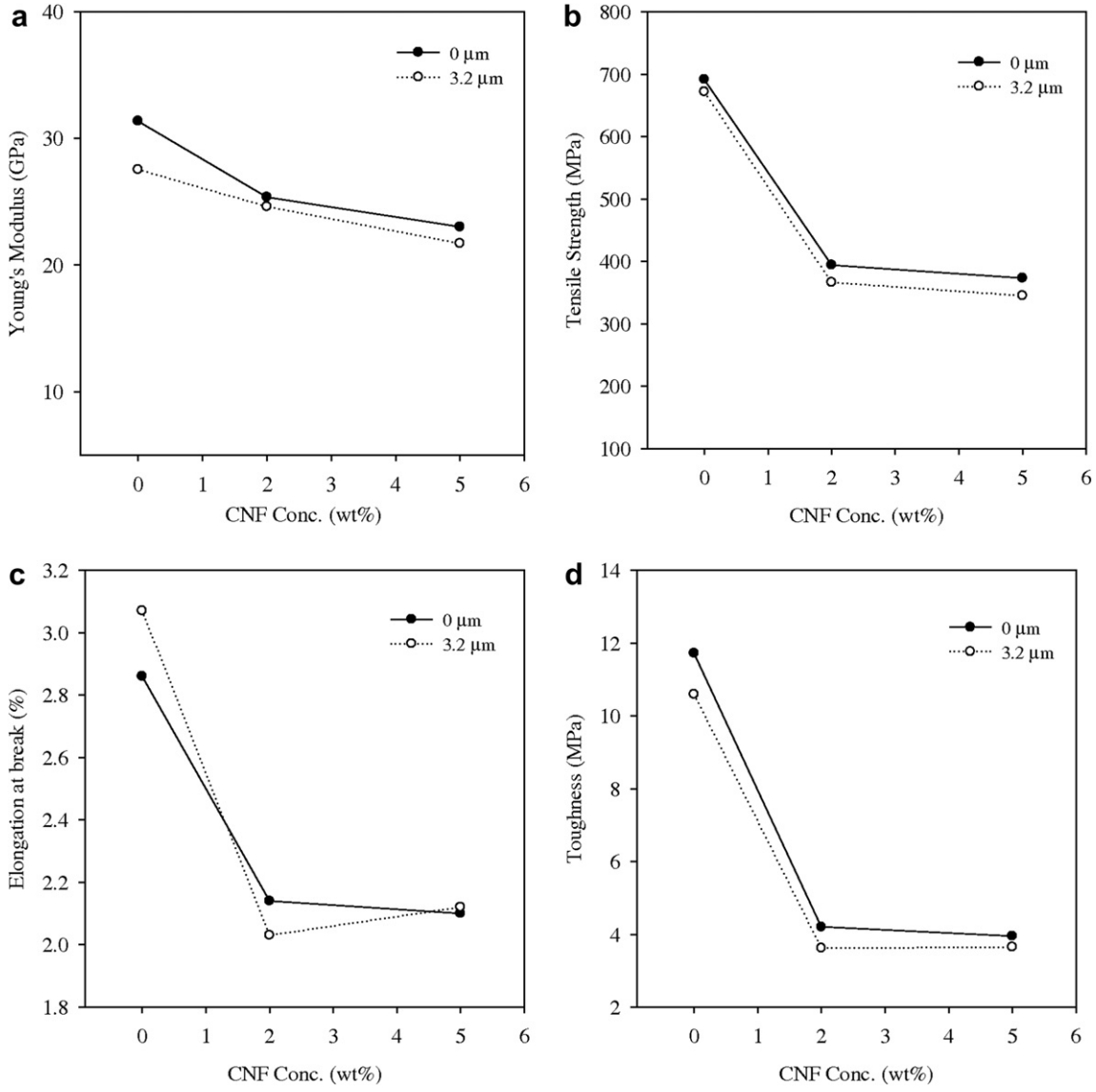

Fig. 10. Young's modulus (a), tensile strength (b), elongation at break (c) and toughness (d) as a function of CNF concentration for melt spun fibers at DDR of 30 without and with ultrasonic treatment at an amplitude of 3.2 μm.

Table 2
Mechanical properties of LCP and LCP/CNF nanocomposite fibers without and with ultrasonic treatment at an amplitude of 3.2 μm and various draw down ratios.

CNF, wt%/μm /DDR	Young's modulus (GPa)	Tensile strength (MPa)	Elongation at break (%)	Toughness (MPa)
0/0/30	31.4 ± 2.7	691.6 ± 87.0	2.86 ± 0.25	11.72 ± 2.84
0/0/51	36.6 ± 1.92	845.2 ± 58.0	2.91 ± 0.20	14.53 ± 1.73
0/0/75	39.7 ± 2.78	864.6 ± 104.7	2.67 ± 0.3	13.18 ± 2.47
0/3.2/30	27.5 ± 3.47	671.9 ± 63.2	3.07 ± 0.17	10.59 ± 1.31
0/3.2/51	30.2 ± 3.01	659.7 ± 66.5	2.44 ± 0.25	10.52 ± 2.12
0/3.2/75	42.8 ± 4.39	960.58 ± 43.0	2.61 ± 0.19	13.31 ± 1.38
2/0/30	25.4 ± 0.64	394.34 ± 47.9	2.14 ± 0.17	4.20 ± 0.82
2/3.2/30	24.6 ± 1.01	366.45 ± 16.7	2.03 ± 0.19	3.62 ± 0.49
2/3.2/51	27.7 ± 2.65	460.95 ± 45.2	2.06 ± 0.28	4.80 ± 1.14
5/0/30	23.0 ± 0.82	373.27 ± 32.3	2.10 ± 0.20	3.95 ± 0.73
5/3.2/30	21.7 ± 1.74	345.13 ± 24.7	2.12 ± 0.19	3.65 ± 0.56
5/3.2/51	20.1 ± 2.83	327.68 ± 52.9	1.83 ± 0.24	3.13 ± 0.92
5/3.2/75	25.4 ± 0.31	426.93 ± 6.72	1.92 ± 0.10	4.20 ± 0.27

higher mechanical properties [9]. Hence, the orientation of CNFs along with the orientation and fibrillation of LCP chains can drastically improve the mechanical properties of the LCP/CNF nanocomposites. However, CNFs on addition to the LCPs in melt state, may hinder the fibrillation process or alignment of the LCP chains along the flow direction and, hence, no improvement in mechanical properties was observed even on an addition of 20 wt% of CNFs. The same behavior was also reported for LCP reinforced with carboxylated MWNTs [15]. On the other hand, due to improved dispersion of the CNFs in a polymer matrix in the present study, the mechanical properties also did not decrease even at such a high CNFs loading, as compared to other study where even addition of even 5 wt% of CNFs showed significant decrease in the mechanical properties [14]. To the best of our knowledge, this is the first study showing no drop in the Young's modulus and tensile strength along with an increase in the elongation at break of LCP/CNF nanocomposite moldings in comparison with those of pure LCP.

A significant improvement in the mechanical properties of CNFs based nanocomposites can be achieved by providing orientation to the CNFs. As discussed above LCPs domains also get oriented in the elongational flow giving rise to the very high mechanical properties. LCP/CNFs nanocomposites were melt spun at different draw ratios to obtain oriented LCP domains and CNFs. The LCP/CNF nanocomposites were drawn only upto 5 wt% of CNFs; higher CNFs loading nanocomposites were difficult to draw due to high viscosity and melt fracture leading to breakup of spin line stream. Therefore, only rod-like strands were obtained. From the Fig. 10, it can be seen that mechanical properties of fibers do get affected with the ultrasound, CNFs loading and with the draw down ratios (DDR) as seen from Table 2.

It can be seen from the result in Table 2, that fiber spinning enhanced the mechanical properties of LCP/CNF nanocomposites by about 4 times at certain DDR in comparison with those of moldings. The Young's modulus of pure LCP fibers at DDR of 75 increased by about 400% in comparison with the moldings (from about 10 GPa to about 40 GPa). The tensile strength of pure LCP fibers at DDR of 75 was also increased in comparison to moldings by over 600% (from about 140 MPa to 865 MPa). It was observed that as the DDR increased the mechanical properties of nanocomposite fibers increased significantly indicating the alignment of the CNFs and LCP domains along the fiber axis. It was also observed that as the CNFs loading increased, the mechanical properties get decreased in the drawn fibers, which again indicates that these small nanoscale fibers hinder the fibrillation process of the LCP domains and, hence, results in lower mechanical properties. The toughness of the LCP/CNF nanocomposite fibers also decreased as the CNF loadings increased. It is because of the increased brittleness of drawn fibers due to increased CNF loading.

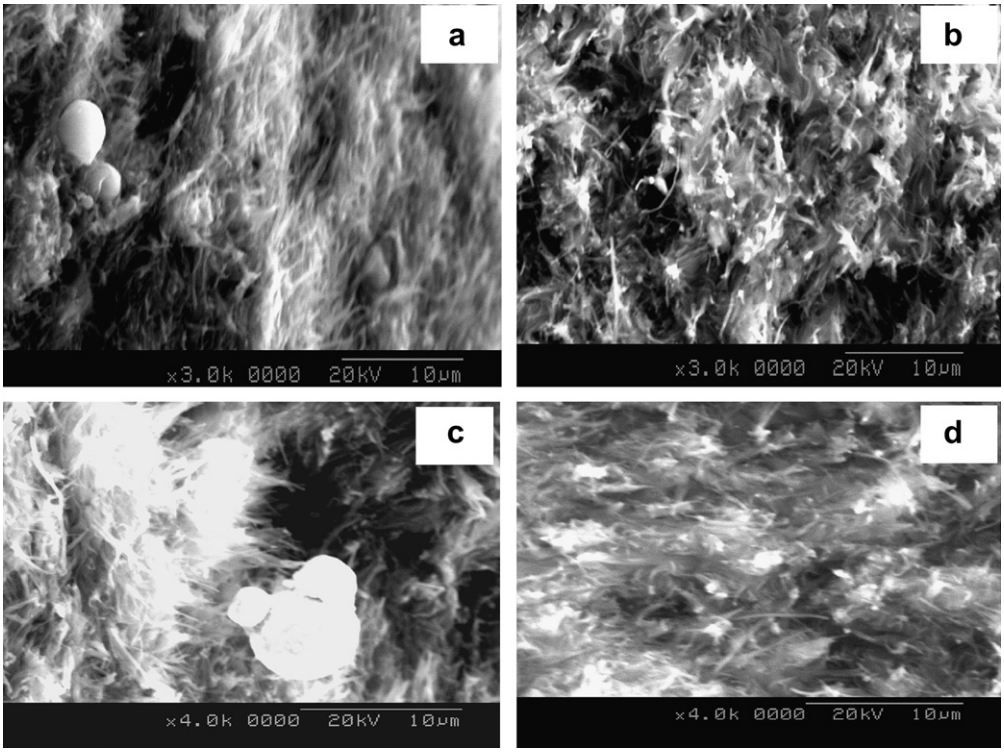

Fig. 11. SEM micrographs of surface of cryofractured moldings at different locations of untreated (a, c) and ultrasonically treated (b, d) LCP/CNF nanocomposites of 20 wt% loading at an amplitude of 3.2 μm.

3.5. Morphology

As received CNFs have large aspect ratio (>100) with diameters varying from 70 to 200 nm. Some catalyst impurity and amorphous carbon may also be present in these samples [11]. The SEM micrograph for as received CNFs reported in Ref. [22] indicated the presence of agglomerated nanofibers in the form of bundles of size ranging from 10 to 50 μm. The disc shape compression molded LCP/CNF nanocomposites for microscopic studies were used. Due to formation of the LCP fibril structure upon injection molding it was difficult to break the injection molded impact bars to get the leveled surface for SEM studies. Fig. 11 shows the SEM micrographs of untreated (a) and ultrasonically treated (b) compression molded nanocomposites filled with 20 wt% CNFs. It is clearly seen from the micrographs that the fibrillation in LCPs is totally destroyed on addition of high loading of CNFs. It is very difficult to distinguish between LCP fibers and CNFs as both look to be of same structure. However, it can be clearly seen that samples ultrasonically treated at an amplitude of 3.2 μm (Fig. 11b) shows that the CNFs are more uniformly distributed across the whole matrix, whereas in case of untreated samples (Fig. 11a) LCP rich areas as big as 4 μm can be observed easily. SEM micrographs were taken at different magnifications and at different places. In case of the untreated samples LCP rich areas as big as 7 μm in size can be seen (Fig. 11c), whereas a uniform distribution of CNFs in the LCP matrix was observed in ultrasonically treated samples without an occurrence of LCP rich areas (Fig. 11d).

4. Conclusions

Ultrasound assisted twin screw extrusion process with separate feeding of CNFs in the melt state was developed for manufacturing LCP/CNF nanocomposites. Ultrasonic treatment caused significant reduction in die pressure. The complex viscosity, storage and loss moduli of LCP/CNF nanocomposites significantly increased with increase of CNF loadings. However, no significant effect was observed upon ultrasonic treatment. Ultrasonically treated samples show lower electrical percolation threshold values than the untreated ones, indicating the better dispersed but interconnected network of CNFs in a polymer matrix. An addition of CNFs in an LCP reduces the fibrillation of matrix. Hence, no significant improvement in the Young's modulus and strength of moldings was observed on an addition of CNFs into the matrix. However, a significant improvement in the elongation at break of moldings was found upon an addition of CNFs to LCP. In comparison to moldings, melt spun fibers of LCP and nanocomposites show tremendous increase in the Young's modulus and tensile strength due to increased orientation of LCP domains and CNFs. In fibers a decrease in mechanical properties was observed on an increase of CNFs content. This indicates the destruction of fibrillar structure of LCP domains due to the presence of CNFs. Hence, this results in reduction in mechanical properties of LCP/CNF fibers. Microscopic studies show that ultrasound does help in improving the uniform dispersion of CNFs in an LCP matrix leading to the elimination of LCP rich areas. In comparison with existing literature available on LCP/CNF nanocomposites showing reduction of mechanical properties upon an addition of CNF or CNT in comparison with those of pure LCP, the present study for the first time shows that mechanical properties can be preserved or improved along with significant improvement of the electrical conductivity.

Acknowledgement

The authors are grateful for the financial support provided by NSF under Grant No. CMMI-0654326.

References

[1] Tibbetts GG, Lake ML, Strong KL, Rice BP. Compos Sci Technol 2007;67:1709.
[2] Barrera EV. JOM 2000;52:38.
[3] Ajayan PM, Schadler LS, Braun PV. Nanocomposite sci & tech. Weinheim: Wiley; 2003.
[4] Zhao J, Schaefer DW, Shi D, Lian J, Brown J, Beaucage G, et al. J Phys Chem B 2005;109:23351.
[5] Higgins BA, Brittain WJ. Eur Polym J 2005;41:10936.
[6] Breuer O, Sundararaj U. Polym Compos 2004;25:630.
[7] Ma H, Zeng J, Realff ML, Kumar S, Schiraldi DA. Compos Sci Technol 2003;63:1617.
[8] Gauthier C, Chazeau L, Prasse T, Cavaille JY. Compos Sci Technol 2005;65:335.
[9] Isayev AI. Chapter 1 in book liquid polymer systems: technological advances. In: Isayev AI, Kyu T, Cheng SZD, editors. ACS symposium series, 632; 1996. p. 1.
[10] Foldberg G, Hedenqvist MS, Gedde UW. Polym Eng Sci 2003;43:1044.
[11] Lozano K, Bonilla J, Barrera EV. J Appl Polym Sci 2001;80:1162.
[12] Zeng J, Saltisyak B, Johnson WS, Schiraldi DA, Kumar S. Compos B Eng 2004;35(2):173.
[13] Lee S, Kim M, Naskar AK, Ogale AA. Polymer 2005;46:2663.
[14] Rohtagi A, Thomas JP, Baucom JN, Pogue WR, Cerully LB, Ebenstein DM, et al. Scripta Mater 2008;58:25.
[15] Park SK, Kim SH, Hwang JT. J Appl Polym Sci 2008;109:388.
[16] Isayev AI, Wong CM, Zeng X. Adv Polym Technol 1990;1990(10):31.
[17] Isayev AI, Chen J. US Patent 5,284,625; 1994.
[18] Isayev AI, Chen J, Tukachinsky A. Rubber Chem Technol 1995;68:267.
[19] Isayev AI, Yushanov SP, Chen J. J Appl Polym Sci 1996;59:815.
[20] Tukachinsky A, Schworm D, Isayev AI. Rubber Chem Technol 1996;69:92.
[21] Feng W, Isayev AI. Polymer 2004;45:1207.
[22] Isayev AI, Jung C, Gunes K, Kumar R. Int Polym Process 2008;23(4):395.
[23] Isayev AI, Kumar R, Lewis T. Polymer 2009;50:250.
[24] Potschke P, Fornes TD, Paul DR. Polymer 2002;43:3247.
[25] McNally T, Potschke P, Halley P, Murphy M, Martin D, Bell SEJ, et al. Polymer 2005;46:8222.
[26] Hu G, Zhao C, Zhang S, Yang M, Wang Z. Polymer 2006;47:480.
[27] Du F, Scogna RC, Zhou W, Brand S, Fischer JE, Winey KI. Macromolecules 2004;37:9048.
[28] Potschke P, Abdel-Goad M, Alig I, Dudkin S, Lellinger D. Polymer 2004;45:886.